Optical spectra of $La_{2-x}Sr_xCuO_4$: Effect of carrier doping on the electronic structure of the CuO_2 plane

S. Uchida
Engineering Research Institute, University of Tokyo, Yayoi, Tokyo 113, Japan

T. Ido and H. Takagi
Department of Applied Physics, University of Tokyo, Hongo, Tokyo 113, Japan

T. Arima and Y. Tokura
Department of Physics, University of Tokyo, Hongo, Tokyo 113, Japan

S. Tajima
Superconducting Research Laboratory, International Superconductivity Technology Center, Shinonome, Tokyo, Japan
(Received 30 August 1990)

Optical reflectivity spectra are studied for single crystals of the prototypical high-T_c system $La_{2-x}Sr_xCuO_4$ over a wide compositional range $0 \le x \le 0.34$, which covers insulating, superconducting, and normal metallic phases. The measurements are made at room temperature over an energy range from 0.004 to 35 eV for the polarization parallel to the CuO_2 planes. They are also extended to the perpendicular polarization to study anisotropy and to discriminate the contribution from the CuO_2 plane. The present study focuses on the x dependence of the optical spectrum, which makes it possible to sort out the features of the excitations in the CuO_2 plane and thus to characterize the electronic structure of the CuO_2 plane in the respective phase. Upon doping into the parent insulator La_2CuO_4 with a charge-transfer energy gap of about 2 eV the spectral weight is rapidly transferred from the charge-transfer excitation to low-energy excitations below 1.5 eV. The low-energy spectrum is apparently composed of two contributions; a Drude-type one peaked at $\omega=0$ and a broad continuum centered in the midinfrared range. The high-T_c superconductivity is realized as doping proceeds and when the transfer of the spectrum weight is saturated. The resulting spectrum in the high-T_c regime is suggestive of a strongly itinerant character of the state in the moderately doped CuO_2 plane while appreciable weight remains in the charge-transfer energy region. The spectrum exhibits a second drastic change for heavy doping ($x \sim 0.25$) corresponding to the superconductor-to-normal-metal transition and becomes close to that of a Fermi liquid. The results are universal for all the known cuprate superconductors including the electron-doped compounds, and they reconcile the dc transport properties with the high-energy spectroscopic results.

I. INTRODUCTION

A two-dimensional sheet of corner-linked CuO_4 squares (CuO_2 plane) is a common structural element of the known high-temperature superconductors. The parent compounds such as La_2CuO_4, $YBa_2Cu_3O_6$, and Nd_2CuO_4 are charge-transfer (CT) insulators with an energy gap between occupied O $2p$ and the lowest unoccupied Cu $3d$ (upper Hubbard) bands.[1] The optical reflectivity (absorption) spectra of these insulating compounds show a pronounced peak at 1.5–2.0 eV, corresponding to the optical transitions across the CT gap.[2] Carrier doping into the CuO_2 plane is expected to change its electronic structure so as to favor high-temperature superconductivity. The accumulated experimental data on the normal-state properties seem "anomalous," in many aspects suggesting the unconventional metallic state realized in the doped CuO_2 plane. The highlights of such anomalous properties would be the apparently conflicting results of the Hall effect[3] and photoemission spectra.[4] The Hall effect suggests a small Fermi surface, corresponding to the dopant concentration x, i.e., x holes per Cu, while the result of the angle-resolved photoemission indicates the existence of a large Fermi surface corresponding to $(1+x)$ holes or $(1-x)$ electrons.[5–7]

The optical measurement is expected to bridge the dc transport property and the high-energy spectroscopy. Important contributions were made from Thomas *et al.*[8] and Collins *et al.*[9] on the $YBa_2Cu_3O_{6+x}$ system. They revealed that the optical conductivity in the low-energy region $\hbar\omega < 1$ eV is not of the usual Drude type, but seems to be composed of at least two components, a Drude-like narrow (with a width of k_BT) band centered at $\omega=0$ and a broadband centered in the midinfrared (mid-IR) region. However, the experiments were restricted to the narrow compositional range, and a quantitative conclusion on the systematic change of the electronic structure is difficult to be drawn owing to the presence of CuO chains which give a substantial contribution to the optical conductivity in the low-energy region.[10,11] More-

over, the charge distribution between CuO chains and CuO_2 planes gives rise to a complicated relationship between the composition x and the actual hole concentration in the CuO_2 plane.[12]

The present optical study is on a series of single crystals of $La_{2-x}Sr_xCuO_4$ grown by a flux-growth method to clarify the carrier doping effect on the electronic structure of the parent CT insulator La_2CuO_4. The advantages of studying $La_{2-x}Sr_xCuO_4$ are twofold: (i) The La system has the simplest crystal structure with a single CuO_2 plane in the structural unit, and the contribution to the optical spectrum below 3 eV is mostly from the CuO_2 plane.[13,14] (ii) The dopant concentration is equal to the Sr composition x and can be varied over a wide range $0 \le x \le 0.34$ without appreciable loss of oxygen content. This compositional range covers the three fundamental phases, the antiferromagnetic insulator, high-T_c superconductor, and nonsuperconducting metal with increasing x. Such successive phase changes are universal in all copper oxide superconductors.

We focus here on the x dependence of the optical spectrum and demonstrate that the spectrum exhibits drastic changes at $x \sim 0$ and ~ 0.25 over a wide energy range up to 3 eV associated with the changes of the electronic structure of the CuO_2 plane. It will be shown that the doping into the insulating CuO_2 plane shifts the spectral weight from high-energy charge-transfer excitation to low-energy excitations, giving rise to an unusual metallic state. The high-T_c regime turns out to be realized when the transfer of the spectral weight is saturated, but appreciable weight persists in the charge-transfer energy range. The second change at $x \sim 0.25$ coincides with the superconductor-to-"normal"-metal transition, and the spectrum of the heavily doped CuO_2 plane turns out to be close to that of a Fermi liquid.

II. EXPERIMENTAL PROCEDURES

A. Sample preparation

Fairly homogeneous large single crystals (typical dimensions $8 \times 5 \times 0.5$ mm^3) have been synthesized for various concentrations of Sr in Pt crucibles by adjusting the starting composition of CuO flux, melting temperature, cooling rate, etc. La_2O_3, $SrCO_3$, and CuO powders were mixed and heated up to 1350°C. They were cooled slowly (5–10 degr C/h) down to 1200 °C and then quenched to room temperature. The starting compositions of these powders were optimized, as indicated in the triangular diagram shown in Fig. 1. The crystals taken out of the flux were post-annealed in flowing oxygen at 900 °C for 25 h and then at 500 °C for 50 h. The crystals with $x \ge 0.10$ were annealed by applying high oxygen pressure of ~ 80 bars for 10–20 h in order to fill possible oxygen vacancies. The highest T_c for the optimum composition $x = 0.15$ is 25 K, about 10 K lower than the best qualified polycrystal.[15,16] Additional or longer-time annealing did not improve the T_c value appreciably. Thus the lower T_c originates not only from oxygen vacancies, but also from other factors, such as contamination from the Pt crucible. Nevertheless, sample homogeneity is satisfactory in

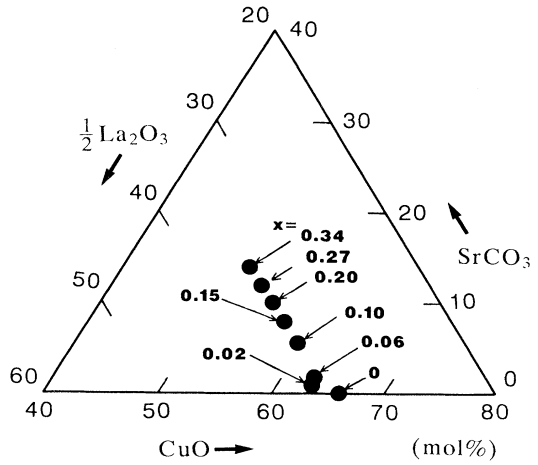

FIG. 1. Triangular diagram for the compositions of the starting materials La_2O_3, $SrCO_3$, and CuO to grow single crystals of $La_{2-x}Sr_xCuO_4$. The optimum compositions for each x are indicated by solid circles.

view of systematic variations of the c-axis lattice constant, the resistivity in the normal state, and the optical spectrum presented here. The electron-probed microscopic analysis with a probing spot of 5 μm in diameter also gives support for homogeneity, the deviation of x from the nominal x being less than $\delta x = 0.01$ for each crystal. The crystals with $x = 0$ and 0.02 are semiconducting—the antiferromagnetic order was observed in the magnetic susceptibility below 280 K for $x = 0$ after being heat treated at 900 °C for 10 h under a reducing atmosphere (10^{-4} atm oxygen partial pressure). The $x = 0.06$ is marginal, some crystals in the same batch exhibiting superconductivity, but the crystal used for optical measurement is semiconducting at low temperatures. Bulk superconductivity is observed for $x = 0.10$, 0.15, and 0.20 with onset $T_c = 18$, 27, and 22 K, respectively. The magnetic measurement at 4.2 K recorded a large Meissner signal (30–100 % for a field of 10 G). The superconducting transition width ΔT_c was 2 K for $x = 0.15$ and 0.20 and $\Delta T_c \sim 5$ K for $x = 0.10$. The samples with $x = 0.27$ and 0.34 do not show superconductivity, but are metallic with much reduced resistivity $\rho \le 2 \times 10^{-4}$ Ω cm at 300 K (see Fig. 2).

B. Optical measurements

The reflectivity spectrum ($\sim 15°$ incident) was measured on the a-b surface (parallel to the CuO_2 planes) in the energy range 4 meV–35 eV using a Fourier-type interferometer (4 meV–1.2 eV), a grating monochromator (0.5–4.0 eV), and a Seya-Namioka-type grating for synchrotron orbital radiation (2–35 eV) at the Institute for Solid State Physics, University of Tokyo. The reflectivity was calibrated with a Au or Al mirror reference in the energy region below 3 eV. The accuracy of the reflectivity is 0.02–0.05 and no calibration due to sample size was necessary because the dimension of sample sur-

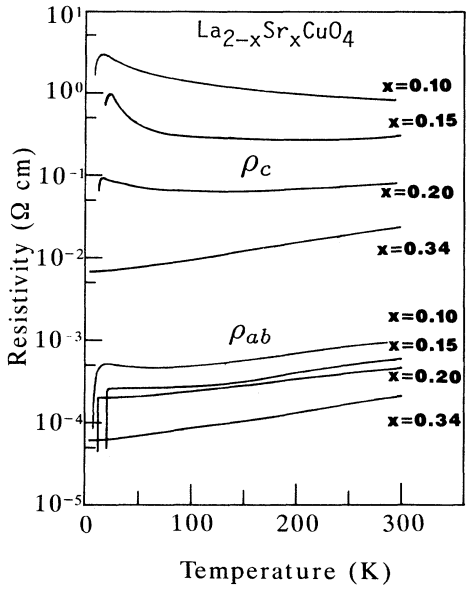

FIG. 2. Temperature dependence of the electrical resistivity for $La_{2-x}Sr_xCuO_4$ single crystals ($x \geq 0.10$) used in this study. Both in-plane (ρ_{ab}) and out-of-plane (ρ_c) data are plotted, which were measured by the Montgomery method. Most of the data for semiconducting crystals ($x \geq 0.06$) scale out of this frame and are not shown.

face was large enough. Additionally, we have checked the reflectivity using a microscopic optical system with a focus of typically 50×50 μm^2 in the energy region between 5 meV and 1 eV. The microscopic measurement also gave a guarantee to homogeneity of the crystals. The same system was also used for the measurement of optical anisotropy with polarization perpendicular to the CuO_2 planes.

One can learn more about the optical response of the oxides from the optical conductivity $\sigma(\omega)$, which is related to the imaginary part of the dielectric function $\epsilon_2(\omega)$ by $\sigma(\omega)=(\omega/4\pi)\epsilon_2(\omega)$. The dielectric function is obtained by the Kramers-Kronig (KK) transformation of the reflectivity $R(\omega)$. Formally, the KK transformation requires a knowledge of $R(\omega)$ at all ω's from 0 to ∞, and so one needs extrapolation of $R(\omega)$ to energies which the measurements cannot cover.

In the present work the higher-energy part ($\hbar\omega > 35$ eV) was smoothly continued by the reflectivity varying as $1/\omega^4$, which is the asymptotic behavior of free electrons. We find that ambiguity arising from the way of continuation does not affect the result at energies of our primary concern, $\hbar\omega < 4$ eV. In the lower-energy region ($\hbar\omega < 4$ meV), we assumed a constant reflectivity for insulating samples $x=0$ and 0.02, since no optical-phonon or substantial free-carrier contribution is expected in this region. On the other hand, for metallic samples the reflectivity was continued by the Hagen-Rubens formula for $x < 0.15$ or by the Drude formula otherwise. The choice of low-energy extrapolation is found not to significantly influence $\sigma(\omega)$ in the region where actual data exist.

The present report is restricted to the data taken at room temperature. A preliminary measurement at low temperatures could not find any significant change in the reflectivity spectrum except for sharpened optical-phonon structures and for only slightly enhanced reflectivity in the far-infrared region (< 25 meV).

III. EXPERIMENTAL RESULTS

A. High-energy spectrum and anisotropy

In Fig. 3 the reflectivity spectrum of La_2CuO_4 is shown to 35 eV for the polarization of the incident light parallel to the CuO_2 planes ($\mathbf{E} \perp c$; we use this convention hereafter). In the same figure is also shown the spectrum for the perpendicular polarization ($\mathbf{E} \| c$). The overall features are commonly observed in almost all the perovskite-related oxide materials; that is, three distinct reflectivity edges appear at ~ 1, ~ 12, and ~ 30 eV. The highest-energy edge originates from the excitations involving all the valence electrons $N_v = 33$ composed of 6×4 O $2p$ valence electrons and 9 Cu $3d$ electrons. The edge corresponds to so-called valence-electron plasma edge. Actually, the reflectivity above 30 eV varies as $1/\omega^4$. A band of relatively high reflectivity starting from 3 eV and ending at the second edge at ~ 12 eV is assigned to the interband excitations from O $2p$ valence bands to the conduction bands of La $5d/4f$ orbitals. In fact, the observed spectrum in this region is in excellent agreement with the band calculational result of Mazin *et al.*,[17] as demonstrated in Fig. 4 where the KK transformed $\mathrm{Im}\epsilon(\omega)$ spectrum is compared with the result of the band calculation.

It follows that the spectrum below 3 eV is dominated by excitations in the CuO_2 plane. The spectrum turns out to be most anisotropic in this energy region. In the $\mathbf{E} \| c$ spectrum no structure corresponds to the 1-eV edge in the $\mathbf{E} \perp c$ spectrum; instead, the low-energy spectrum is

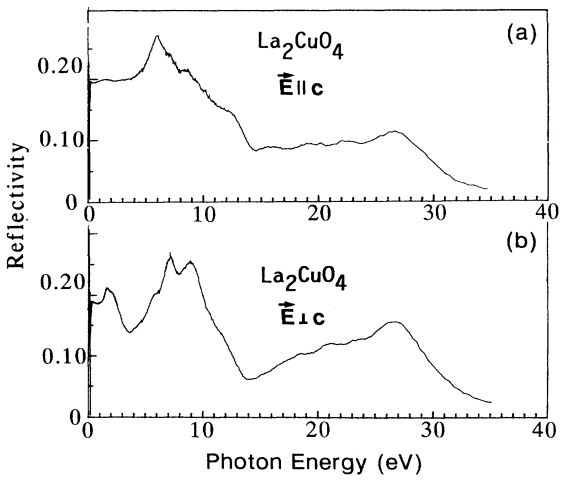

FIG. 3. Reflectivity spectra of La_2CuO_4 measured up to 35 eV for polarization (a) $E \| c$ and (b) $E \perp c$.

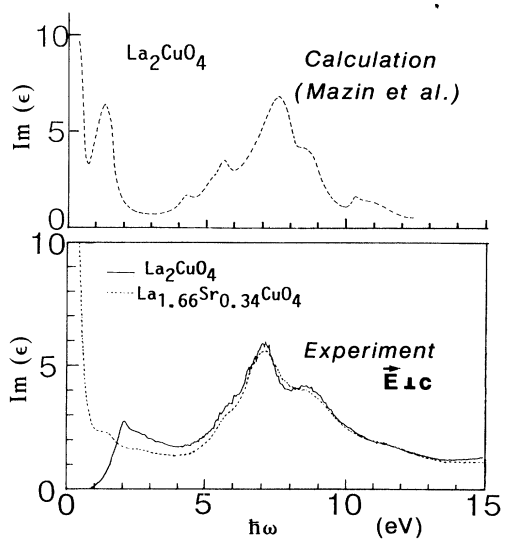

FIG. 4. Comparison of the imaginary part of the dielectric function $\mathrm{Im}\epsilon(\omega)$ between the band calculational result of Mazin *et al.* (Ref. 17) for La_2CuO_4 and the present experimental results obtained from a Kramers-Kronig transformation of the reflectivity. The experimental data for a heavily doped crystal, $x=0.34$ (dotted curve), shows a remarkable change below 5 eV, while no appreciable change is expected in the calculational result for Sr-substituted La_2CuO_4.

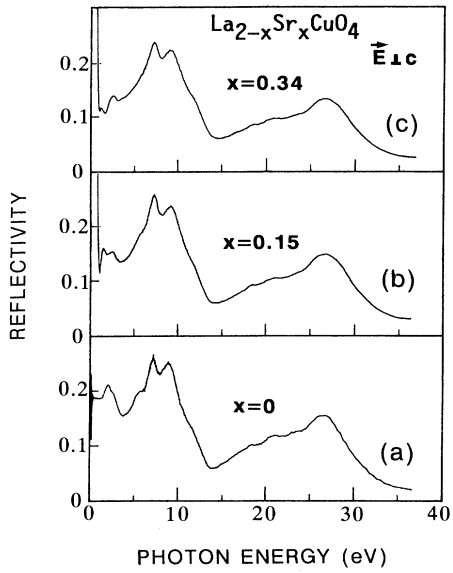

FIG. 5. Reflectivity spectra ($E \perp c$) for three representative compositions (a) $x=0$, (b) 0.15, and (c) 0.34 of $La_{2-x}Sr_xCuO_4$ single crystals.

dominated by optical phonons as will be shown later. The presence or otherwise of this edge is an indication of the metallic state along CuO_2 planes or a semiconducting one across the planes, respectively. By contrast, higher-energy spectral features are very similar except for a few weak structures, which should be ascribed to the optical transitions at different wave vectors in the same bands. As expected from the anisotropic crystal structure, a quasi-two-dimensional character of the electronic state manifests itself in the low-energy excitations which are taking place in the CuO_2 plane.

B. Spectrum of undoped La_2CuO_4

The reflectivity spectrum ($\mathbf{E} \perp c$) of the parent compound La_2CuO_4 is shown again in Fig. 5(a). While the spectrum above 3 eV is almost the same as that for doped compound, it is drastically different in the low-energy region. The spectrum of the as-grown crystal exhibits a trace of the 1-eV edge, which arises from a slight amount of holes provided by excess oxygens in the crystal. However, after annealing at 650 °C under a reducing atmosphere, the edge disappears and the spectrum is characterized by a peak at 2 eV as well as by three optical-phonon bands below 0.1 eV. The spectrum is almost flat and featureless between these energies.

The 2-eV peak is assigned to O $2p \rightarrow$Cu $3d$ (upper Hubbard band) CT excitation within the CuO_2 plane from the experimental fact that it sets up an optical energy gap of insulating La_2CuO_4 and it is not seen in the spectrum for the light polarized perpendicular to the CuO_2 planes. It is commonly observed in the spectra for other insulating layered cuprates such as Nd_2CuO_4, $YBa_2Cu_3O_6$, $CaCuO_2$ etc. In a previous paper[2] we reported that the corresponding peak is located at an energy between 1.5 and 2.0 eV for all the materials investigated so far. A difference was ascribed to the difference in the oxygen coordination number surrounding Cu. In fact, the peak energy is higher for compound with more apical oxygens: 2.0 eV for T-phase La_2Cu_4, 1.7 eV for T^*-phase $LaDyCuO_4$, and 1.5 eV for T'-phase Nd_2CuO_4.

C. Doping effect

1. *Reflectivity spectrum*

Substitution of Sr for La makes no significant change in the spectrum above 4 eV as demonstrated in Figs. 5(b) and 5(c) for the representative compositions $x=0.15$ and 0.34. By contrast, the spectrum in the lower-energy region exhibits drastic changes with doping. The reflectivity spectra are shown in Fig. 6 for various Sr compositions. With small amount of Sr substitution, the reflectivity of the CT peak is severely reduced; instead, a reflectivity edge suddenly appears at ~ 0.8 eV. As doping proceeds, the reflectivity edge becomes sharpened and the reflectivity below the edge rapidly increases. As a consequence, three optical-phonon bands still seen in the spectrum of $x=0.06$ are screened out for $x \geq 0.10$. It is noteworthy that the position of the edge does not shift appreciably with doping. The shift becomes appreciable only for heavy doping $x > 0.25$. However, the edge moves to lower energy which is in the direction opposite to what one expects from the increased hole concentration.

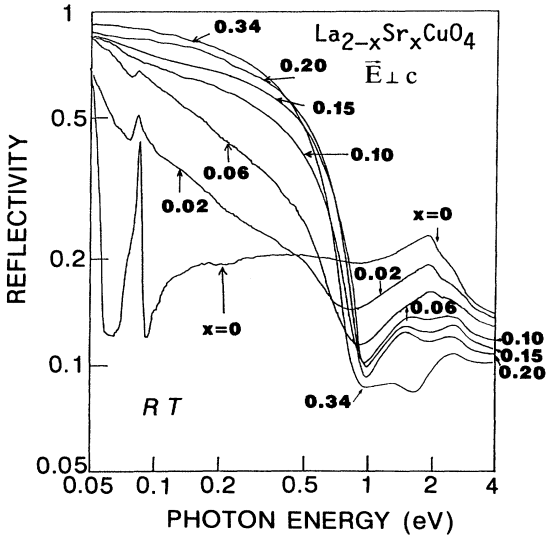

FIG. 6. Reflectivity spectra below 4 eV for various compositions of $La_{2-x}Sr_xCuO_4$ single crystals measured at room temperature (RT) with polarization parallel to the CuO_2 planes. Both reflectivity and photon energy are shown in logarithmic scales.

2. *Optical conductivity*

We can learn from the optical conductivity more about what is happening on doping. Figure 7 clearly demonstrates that the conductivity rapidly decreases in the energy region above 1.5 eV, while it increases below 1.5 eV. In the former region the CT excitation dominates and the latter involves a free-carrier contribution. However, it cannot be concluded that the free-carrier contribution extends up to 1.5 eV and occupies the entire region below 1.5 eV. Apparently, $\sigma(\omega)$ has two components for lightly doped compounds, a narrow band peaked at $\omega=0$ and a broadband centered in the midinfrared region. Even for moderately and heavily doped compounds, $\sigma(\omega)$ decays much more slowly than the Drude-type ω^{-2} dependence. The, infrared conductivity with two or more components was previously reported for the $YBa_2Cu_3O_{6+x}$ system.[8,18]

In the $\sigma(\omega)$ spectra for $x > 0.10$, two weak features are apparent at 1.5 and 3.0 eV. The 3.0-eV feature is probably intrinsic, which would be overlapped with more dominant CT excitation for small x, but become apparent owing to the suppressed CT excitation for large x. Its origin is not obvious, but perhaps corresponds to the interband excitation to La $5d/4f$ or Cu $4s/4p$ derived conduction bands. The presence of the 1.5-eV peak was reported by Suzuki in his work on thin films of $La_{2-x}Sr_xCuO_4$.[19] In the thin-film spectrum the 1.5-eV absorption peak develops with x, and so he speculated that it might be related to the change of the electronic structure, i.e., the appearance of impurity states within the CT energy gap. The present result on bulk single crystals, however, shows that the 1.5-eV feature is relatively weak and becomes apparent only for $x > 0.10$. Possibly, the 1.5-eV feature is exaggerated or magnified in the thin-film spectrum, either reflection or transmission, since the material is rather transparent in the energy region above the reflectivity edge so that weak absorption is intensified as a result of multiple reflection. Since the corresponding feature is not seen in the spectra for other cuprate systems, we suppose that the 1.5-eV absorption is extrinsic in origin as a result, possibly, of an undetectable amount of oxygen vacancies inevitably present at high Sr compositions. If it were not, the 1.5 eV would be an isosbestic point in a strict sense at which $\sigma(\omega)$ is invariant against x. A beautiful isosbestic behavior is actually observed in electron-doped $Nd_{2-x}Ce_xCuO_4$ as reproduced in Fig. 8.[3] The presence of the isosbestic point in-

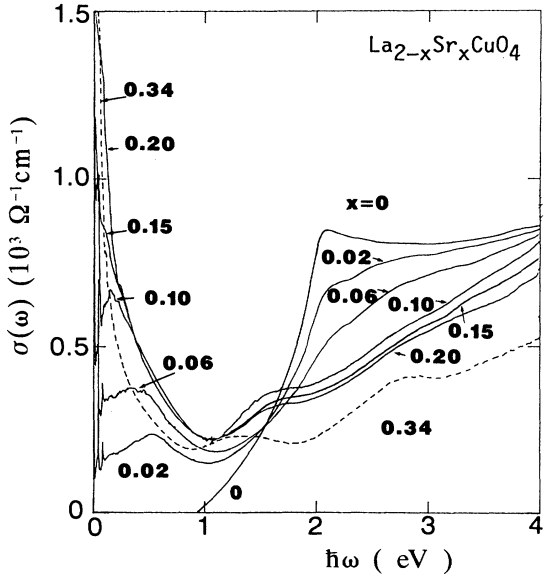

FIG. 7. Optical conductivity $\sigma(\omega)$ obtained from the Kramers-Kronig transformation of the $E \perp c$ reflectivity spectra for various compositions x.

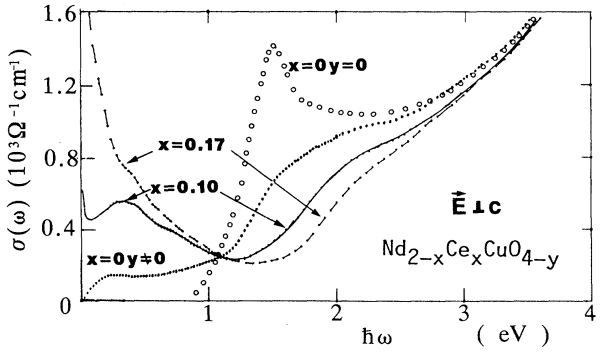

FIG. 8. Optical conductivity spectra ($E \perp c$) of electron-doped $Nd_{2-x}Ce_xCuO_{4-y}$ single crystals with the a-b plane. The spectra show an isosbestic point at 1.1 eV, where $\sigma(\omega)$ becomes equal for any dopant concentration. The data labeled with ($x=0$, $y\neq0$) is for a reduced Nd_2CuO_4 which contains a smaller number of electrons, not specified, supplied by oxygen vacancies.

dicates that the low-energy conductivity is induced by the shift of the spectral weight from the high-energy part.

The transfer of the spectral weight persists up to $x=0.20$, and as a result, the high-energy part, the CT excitation, is severely depressed. In the low-energy region the narrow-band component develops and the peak of the broadband one shifts to lower energy with increasing x. Accordingly, the separation into these two components becomes nontrivial. When x exceeds 0.25 and the compound becomes nonsuperconducting, $\sigma(\omega)$ decreases over a wide energy range, suggesting another radical change of the electronic state in the heavily doped region. Even in this computational region, the conductivity in the lowest-energy part continues to increase, in agreement with the continuous decrease in the dc resistivity.

3. *Energy-loss function*

Returning to the reflectivity spectra, the appearance of a reflectivity edge implies the presence of a peak in the loss function $\mathrm{Im}[-1/\epsilon(\omega)]$. The loss function can also be obtained by the KK transformation on the reflectivity data. The result below 1.5 eV is shown in Fig. 9(a) for several compositions. The value of $\mathrm{Im}(-1/\epsilon)$ for La_2CuO_4 is vanishingly small below 1 eV except in the optical-phonon region, which is omitted from the figure. A weak tail starting from 1 eV is a precursor of the CT excitation, which makes a peak in $\mathrm{Im}(-1/\epsilon)$ at ~ 3 eV. With slight doping a featureless continuum appears in the mid-IR region. This reminds us of the anomalous continuum observed in the same energy range in the electronic Raman-scattering spectrum.[20] The Raman spectra measured by Sugai *et al.* on the same set of crystals are shown in Fig. 9(c) together with the $\mathrm{Im}[1/\epsilon(\omega)]$ spectra. The Raman response function is directly related to $\mathrm{Im}[1/\epsilon(\omega)]$ spectra. The Raman response function is directly related to $\mathrm{Im}(-1/\epsilon)$ in the small momentum-transfer limit

As doping proceeds, a broad peak emerges at ~ 0.8 eV. For superconducting compositions $x=0.10$ and 0.20, the peak is still so broad that it is comparable to the peak energy. It should be noted that such a peak is not seen in the Raman spectrum of the superconducting compound where the electronic contribution maintains a featureless continuum and its intensity decreases with x. The $\mathrm{Im}(-1/\epsilon)$ spectrum qualitatively changes for heavy doping, exhibiting a rather well-defined peak typical of a plasmon peak in a usual metal. The electronic Raman continuum still remains, but is greatly suppressed as compared with smaller compositions.

4. *Effective electron number*

For a next step, in order to give a quantitative basis to the conductivity data, we have estimated the effective electron number (per Cu atom) defined below as a form of the spectral weight up to an energy $\hbar\omega$:

$$N_{\mathrm{eff}}^{*}(\omega)=\frac{2m_0V}{\pi e^2}\int_0^{\omega}\sigma(\omega')d\omega' , \qquad (1)$$

where m_0 is taken as the free-electron mass and V is the

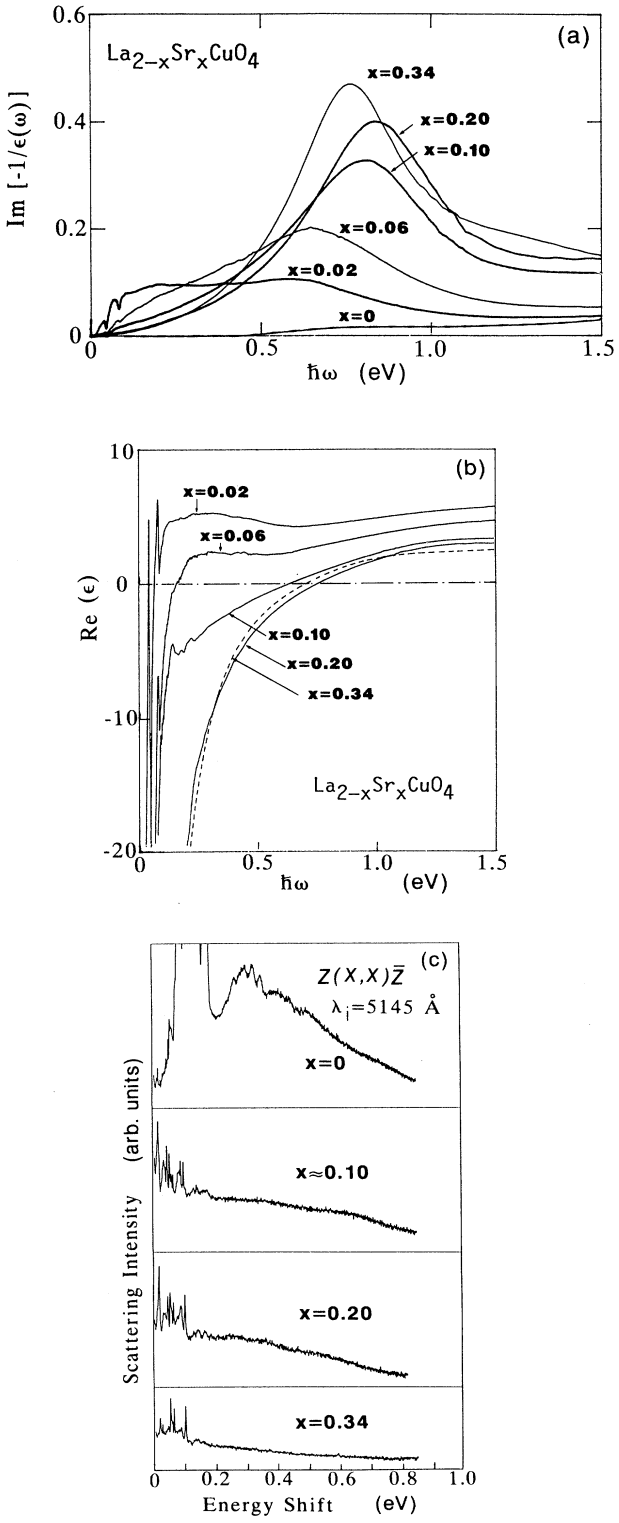

FIG. 9. (a) Energy-loss function $\mathrm{Im}[-1/\epsilon(\omega)]$ and (b) the real part of the dielectric function obtained from the Kramers-Kronig transformation of the reflectivity data. The data below 1.5 eV are shown to focus on the ω dependences near the reflectivity edge (~ 0.8 eV). (c) The A_{1g} Raman spectra with $z(x,x)z$ polarization and incident laser wavelength $\lambda_i=5145$ Å for *a-b* surface single crystals measured by Sugai *et al.* (Ref. 20).

cell volume containing one formula unit. $N^*_{\rm eff}(\omega)$ is proportional to the number of electrons involved in the optical excitations up to $\hbar\omega$. $N^*_{\rm eff}(\omega)$ calculated from the conductivity data are shown in Fig. 10 for various Sr compositions. For $x=0$ contributions from the optical phonons are very small, so that $N^*_{\rm eff}$ becomes appreciable above 1 eV where the absorption band of the CT excitation starts. For doped samples the initial steep rise of $N^*_{\rm eff}$ is due to the narrow band peaked at $\omega=0$, and $N^*_{\rm eff}$ attains substantial values in the mid-IR region. As has been learned from the $\sigma(\omega)$ spectra, most contributions come from the broadband absorption in the mid-IR region, which is also responsible for the reflectivity edge at $\sim$0.8 eV. The substantial part of the low-energy excitations ends up to this edge position (but practically extends up to 1.5 eV), so that $N^*_{\rm eff}$ exhibits a plateau in the interval between 0.8 and 1.5 eV. Above 1.5 eV the remaining CT excitation and high-energy interband transitions contribute to $N^*_{\rm eff}$.

We focus on the values of $N^*_{\rm eff}$ at two characteristic energies obvious in Fig. 10. One is 3.0 eV where $N^*_{\rm eff}$ becomes almost independent of x for $x \leq 0.2$ This gives quantitative evidence that the doping affects the electronic excitations below 3 eV, which presumably represent the spectral weight of the CT excitation for $x=0$ and transfer spectral weight between 1.5 and 3.0 eV to the low-energy excitations below 1.5 eV. Note that $N^*_{\rm eff}$ at 3.0 eV is 0.45 by a factor of 2 smaller than one electron per Cu, which should be involved in the Cu-O CT excitation. The small value or reduced spectral weight might be ascribed to the renormalization due to Coulomb interactions; that is, one should replace m_0 by an effective mass $m^* \sim 2m_0$ in Eq. (1). As a matter of fact, the spectral weight associated with the CT excitation is material dependent—in terms of $N^*_{\rm eff}$ it is 0.50 for T^*-phase $LaDyCuO_4$ and 0.70 for T'-phase Nd_2CuO_4.[2]

Obviously, 1.5 eV is another characteristic energy. As seen in Fig. 7, $\sigma(\omega)$ exhibits nearly isosbestic behavior at 1.5 eV, so that $N^*_{\rm eff}$ (1.5 eV) can be regarded as the spectral weight of low-energy excitations transferred from the CT excitation by doping. The x dependence of $N^*_{\rm eff}$ (1.5 eV), shown in Fig. 11, reveals a remarkable and anomalous doping effect. $N^*_{\rm eff}$ sets in with very slight doping and increases with x at the rate much faster than what one expects from the dopant concentration, i.e., $N^*_{\rm eff} \gg x$. It should be emphasized that $N^*_{\rm eff}$ (1.5 eV) almost stops to increase at $x=0.10$ and is nearly constant in the interval between $x=0.1$ and 0.2, which, incidentally, coincides with the compositional range of bulk high-T_c superconductivity. Although the transfer of the spectra weight from the CT excitation is saturated in this compositional range, the increase of doping biases the spectral weight more onto the lower-energy region.

Heavy doping ($x > 0.25$) decreases $N^*_{\rm eff}$ over a wide energy range. The decrease in the value of $N^*_{\rm eff}$ (1.5 eV) is in accordance with the low-energy shift of the reflectivity edge. The value at 3.0 eV also decreases, which has been

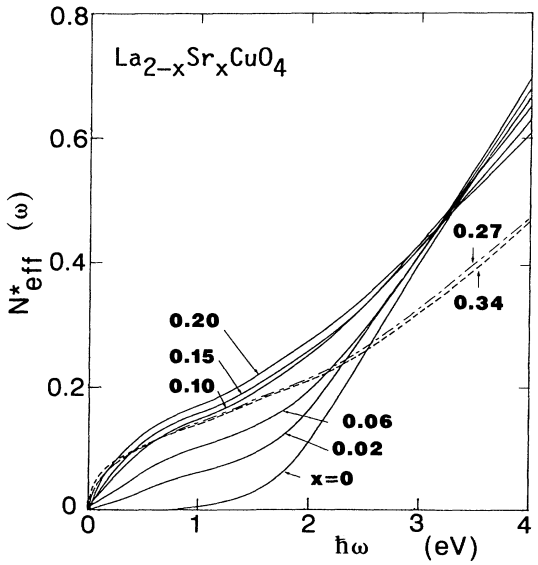

FIG. 10. Effective electron number per Cu atom defined as a conductivity sum is plotted as a function of energy for various compositions. For clarity the data for heavily doped samples, $x=0.27$ and 0.34, are shown by dot-dashed and dashed curves, respectively.

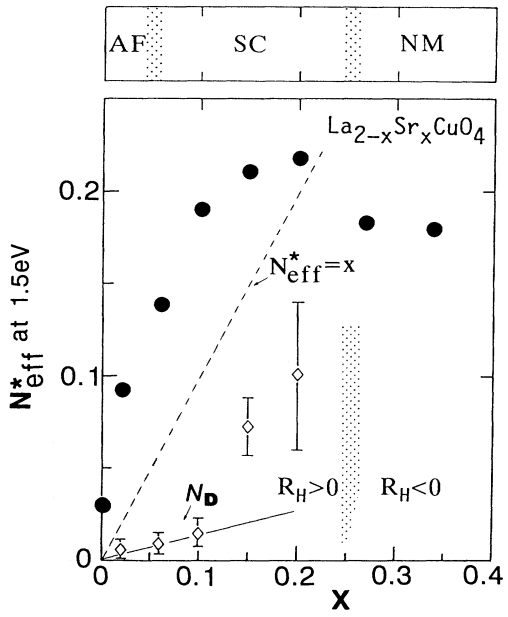

FIG. 11. Effective electron number at 1.5 eV (solid circles) as a function of composition x. The dashed straight line indicates a reference for $N^*_{\rm eff}=x$. The phase boundaries of the antiferromagnetic insulator (AF), superconductor (SC), and normal metal (NM) are shown above. The open diamond with an error bar represents a free-carrier contribution N_D, estimated from a Drude fit to $\sigma(\omega)$ in the lowest-energy part. N_D seems to increase proportionally with x for small x (the line is a guide for the eyes). However, the definition of N_D becomes ambiguous with increasing x, as $\sigma(\omega)$ exhibits a decrease slower than the Drude-type $1/\omega^2$ over almost the entire energy range.

an invariant for smaller compositions. As we have seen, the CT excitation is further suppressed in the heavily doped region, and therefore the result implies that the CT spectral weight is distributed over a wider energy range not restricted below 1.5 eV.

5. *Anisotropy*

As in the case of $\mathbf{E}\perp c$ spectrum, the $\mathbf{E}\|c$ spectrum for $x=0$ is featureless below 4 eV except in the far-infrared region (<0.06 eV) where three optical phonons with A_{2u} symmetry dominate. The spectrum is thus typical of an insulator. Different from the $\mathbf{E}\perp c$ case, doping does not change the $\mathbf{E}\|c$ spectrum substantially even in the low-energy region. In Fig. 12 are shown the spectra for three representative compositions in the far- and mid-IR regions. It turns out that the optical phonons dominate even for superconducting compositions, which is evidence for a semiconducting character in the direction perpendicular to the CuO_2 planes, in contrast to the metallic one parallel to them. Actually, observed the dc resistivity along the c axis increases with lowering temperature[21] (see Fig. 2).

Only when x is in the normal metallic phase does the $\mathbf{E}\|c$ spectrum appear to change qualitatively. Though the highest-energy phonon (~ 70 meV) is not completely screened, the spectrum is apparently affected by free-carrier plasma, as evidenced from shallowed dips at ~ 60 and ~ 80 meV. This is in agreement with the metallic temperature dependence of the resistivity along the c axis for the samples with $x>0.25$. The heavily doped $La_{2-x}Sr_xCuO_4$ might thus be regarded as an anisotropic three-dimensional metal as expected from the band calculational results.[17,22]

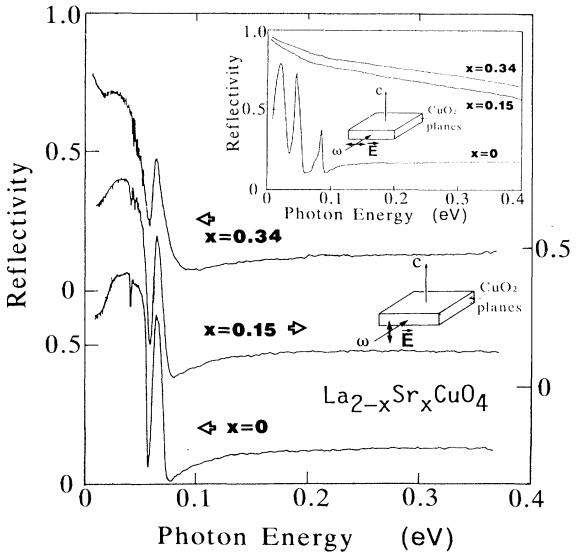

FIG. 12. Reflectivity spectra of three representative compositions for the incident light polarized parallel to the c axis. Three optical-phonon bands below 0.1 eV dominate in the spectrum of La_2CuO_4. The reflectivity measured on the identical surface with $\mathbf{E}\perp c$ polarization is shown in the inset.

IV. DISCUSSIONS

A. Electronic structure of the undoped CuO_2 plane

Figure 4 compares the observed conductivity spectrum of La_2CuO_4 with the available result of the band calculation by Mazin *et al.*[17] The agreement between them turns out to be excellent in the energy region above 4 eV, where the contribution from O $2p\rightarrow$La $5d/4f$ interband transitions dominates. In the lower-energy region the calculated spectrum is characterized by two excitations: One is intraband contribution centered at $\omega=0$ within the half-filled Cu $3d_{x^2-y^2}$–O $2p_{x,y}$ antibonding conduction band, and the other is the interband one between antibonding Cu $3d_{z^2}$–O $2p$ and Cu $3d_{x^2-y^2}$–O $2p$ bands which exhibit a peak at 1.5 eV. However, the corresponding absorptions cannot be seen in the spectrum of real La_2CuO_4. There should be no intraband contribution in insulating La_2CuO_4, and instead of a $d_{z^2}\rightarrow d_{x^2-y^2}$ interband transition, the O $2p\rightarrow$Cu $3d_{x^2-y^2}$ CT excitation is observed peaked at 2.0 eV. This is further evidenced by the fact that, while the O $2p$ hybridized $d_{z^2}\rightarrow d_{x^2-y^2}$ transition is not appreciably affected by doping, the observed 2-eV peak is severely weakened by a small amount of doping. In this regard Fig. 4 is a clear demonstration that band theory cannot describe the low-energy excitation within CuO_2 plane, whereas it nicely mimics the higher-energy interband transition.

The present result, as well as the results on other insulating cuprates, has shown that the undoped CuO_2 plane is a CT insulator with a fundamental optical energy gap ($\Delta\sim 1.5$–2.0 eV) between O $2p$ and Cu $3d$ bands as pictured in Fig. 13(b). This conclusion is consistent with the one drawn from the photoemission experiment.[1] The topmost Cu $3d$ state, $d_{x^2-y^2}$ orbital, is split into Hubbard bands owing to large on-site Coulmb repulsive energy, and as a result, an occupied O $2p$ band is located in be-

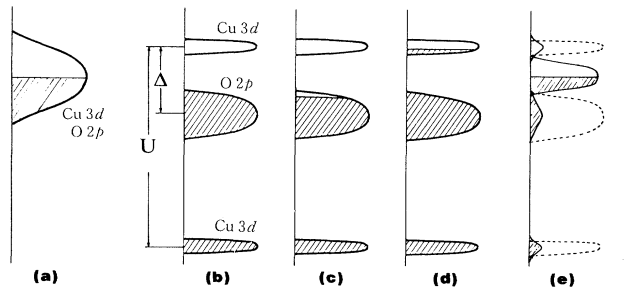

FIG. 13. Schematic energy diagrams for doped and undoped CuO_2 planes. (a) Band picture for a half-filled (undoped) CuO_2 plane (Fermi liquid). (b) Charge-transfer insulating state of the undoped CuO_2 plane with split Cu $3d$ bands due to on-site Coulomb repulsive interaction U. The O $2p$ band is separated by a charge-transfer energy Δ from the upper Cu $3d$ band. (c) and (d) show rigid CT energy bands doped with holes and electrons, respectively. (e) An image of the doped CuO_2 plane inferred from the present study with (midgap) states reconstructed from split O $2p$ and Cu $3d$ orbitals in the CT insulating state.

tween. In this energy scheme the optical CT excitation is a transition from an occupied O $2p$ band to an empty upper Cu $3d$ Hubbard band.

We should here remark on the strength or spectral weight of the CT excitation, as briefly described before. The CT strength considerably differs among various known cuprates—strongest for T'-phase Nd_2CuO_4 and weakest for T-phase La_2CuO_4. We previously measured the optical spectra of non-Cu oxides with K_2NiF_4 structure, La_2NiO_4, La_2CuO_4, and La_2FeO_4, which are all thought to be CT insulators.[13] It was found that their spectra above 5 eV are essentially the same as that for La_2CuO_4, providing convincing evidence for the O $2p \rightarrow$ La $5d/4f$ transitions. However, only very weak features were observed below 4 eV. Thus the CT excitation has very small spectral weight in these non-Cu oxides. The primary reason for weak oscillator strength might be either a larger CT energy gap Δ or smaller transfer energy t between oxygen and transition-metal elements. Roughly speaking, the CT strength is proportional to t^2/Δ for $\Delta \gg t$.

B. Doped CuO_2 plane

The present work demonstrates that the doping into the CuO_2 plane shifts the spectral weight from the CT excitation to low-energy excitations below 1.5 eV. This indicates that the states O $2p$ and Cu $3d$, originally separated by a CT energy gap, are redistributed by doping on a large energy scale, or in other words, a new state is reconstructed from these two orbitals. Thus the doping has a much more radical effect on the electronic structure of the CuO_2 plane than it does on usual semiconductors where the valence band is occupied by holes or impurity states are formed within the gap. Consequently, an energy diagram as depicted in Fig. 13(c), where doped holes occupy the O $2p$ valence band, does not give the entire picture of the doped CuO_2 plane.

We suppose that Fig. 13(c) is correct as far as the lowest-energy excitation in the lightly doped compound is concerned. The infrared conductivity for $x < 0.10$ is apparently composed of two separate contributions, one showing a narrow peak at $\omega = 0$ and a broadband extending over the mid-IR region. In order to estimate the spectral weight of each contribution, the low-energy part of $\sigma(\omega)$ is approximated with a Drude-type oscillator. The spectral weight of this component, N_D, in units of electron number per Cu atom, is plotted in Fig. 11. The difference between $N_{\rm eff}^*$ (1.5 eV) and N_D then gives a contribution from the broadband in the mid-IR region. We expect that thus estimated N_D represents a fully itinerant degree of freedom for doped holes in view of the fact that it is well approximated by the Drude formula. N_D shows an increase roughly proportional to the dopant concentration x for $x < 0.10$, but N_D is much smaller than the value x. If the difference between N_D and x is ascribed to a large enhanced mass $\sim 8m_0$, this is in agreement with the result of the Hall effect. The density of hole carriers estimated from the Hall coefficient roughly coincides with the dopant concentration for small x.[3,15]

Turning to the broadband contribution which occupies the most part of low-energy spectral weight, it exhibits an initial steep increase for very light doping. The increase is associated with the suppression of the CT spectral weight. This implies a redistribution of the states so that they fill up the CT energy gap to produce the low-energy excitations including the mid-IR one. Note that the change induced by doping is not the narrowing of the CT gap, but the reconstruction of the states on a large energy scale by transferring the states from both conduction and valence bands of the parent insulator, as schematically shown in Fig. 13(e). We have seen a sudden onset of the reflectivity edge at 0.8 eV on doping, which is independent of the edge at ~ 3 eV associated with the CT excitation. This observation is reconciled with the reconstruction of new states and is suggestive of a large "Fermi surface" being progressively built up in contrast to a small Fermi surface presumed from the lowest-energy Drude-type excitation.

High-temperature superconductivity takes place in the moderately doped CuO_2 plane ($0.05 < x < 0.25$). In this compositional range the transfer of the spectral weight from the CT excitation exhibits a saturation, but it does not mean that the CT spectral weight is fully transferred. $N_{\rm eff}^*(\omega)$ is still increasing over an energy range above 1.5 eV, indicating that appreciable spectral weight remained in the CT energy region. In this sense the high-T_c regime is a quasiequilibrium state before the CT excitation completely collapses. The characteristic spectral feature in this regime is that the spectral intensity is biased on the lower-energy part because of a developed Drude-type component and the low-energy shift of the mid-IR peak. As a consequence, it becomes difficult to estimate each contribution separately, and the picture of a doped semiconductor such as in Fig. 13(c) is no more valid even from the viewpoint focused on the lowest-energy excitation. In fact, the values of the reciprocal Hall coefficient are significantly larger than expected from the dopant concentration,[3,15] suggesting that more degrees of freedom than x holes take part in the dc transport. Thus a picture like Fig. 13(e), representing a large Fermi surface, becomes prevailing in the high-T_c regime. Although a Fermi liquid, like Fig. 13(a), would be a limiting case of Fig. 13(e), the actual state seems quite unconventional. The Drude formula, even in its generalized form,[23] can never fit the observed $\sigma(\omega)$ spectrum because the contribution corresponding to the mid-IR component for light doping remains as a shoulder or a long tail extending over 1 eV. Also, a trace of the CT excitation remains in the higher-energy region, as deduced from the ω dependence of $N_{\rm eff}^*$. Considering that the CT excitation represents a localized aspect of the electronic state, whereas the low-energy excitations represent, more or less, itinerancy, the electronic state in the high-T_c regime appears to preserve both itinerant and localized character. Recent neutron-scattering experiments[24,25] also suggest the persistence of dynamical antiferromagnetic correlation in this regime.

More evidence for an unconventional metallic state would be its anisotropic spectrum shown in Figs. 3 and 12, which indicate that the low-lying excitations are confined within the CuO_2 plane. The $E \| c$ spectrum, as

well as the temperature dependence of the electrical resistivity (Fig. 2), clearly shows semiconducting character across the CuO_2 planes, while the band calculation predicts a metallic state in any direction.[22] It is not allowed in the conventional localization theory that the system is metallic in one direction but nonmetallic in another.[26]

We should further remark that essentially the same spectral change has been reported for hole doping into $YBa_2Cu_3O_{6+x}$ (Ref. 27) and $Bi_2Sr_2Y_{1-x}Ca_xCu_2O_8$,[28] though the measurement is restricted to narrower range of dopant concentration. In addition, as shown in Fig. 12 for electron-doped $Nd_{2-x}Ce_xCuO_4$, doping electrons into the CuO_2 plane is expected to convert the CT insulating state into a state similar to that realized by hole doping.[3] Therefore, as far as the electronic structure of the doped CuO_2 plane is concerned, electron-hole symmetry seems to hold as in the Hubbard model or in the picture of exactly half-filled band.

C. Heavily doped CuO_2 plane

A drastic change of the optical spectrum occurring at $x \sim 0.25$ suggests a qualitatively different electron structure in the heavily doped CuO_2 plane which does not superconduct. The CT excitation or energy gap seems almost collapsed, and the states near the Fermi energy, probably both Cu $3d$ and O $2p$, appear to achieve full itinerancy. Actually, the real part of the dielectric function crosses zero at $\omega=\omega_p \sim 0.7$ eV, where the reflectivity exhibits an edge and the loss function $\mathrm{Im}[-1/\epsilon(\omega)]$ shows a well-defined peak at ω_p, as shown previously in Fig. 9. There are typical characteristics of usual metals. In addition, the $\mathbf{E}\|c$ spectrum suggests metallic, though poorly metallic, character along the c axis as expected from the band calculation.[22] The $\sigma(\omega)$ spectrum below 1 eV, however, does not fit the sample Drude formula because the observed $\sigma(\omega)$ has a tail decaying slower than the Drude type ω^{-2} dependence. Nevertheless one can simulate $\sigma(\omega)$ with a generalized Drude formula by assuming reasonable ω dependences of the scattering rate $\tau^{-1}(\omega)$ and its KK transform $m^*(\omega)$, the effective mass, like the case of heavy-fermion superconductors.[23] The estimated $\tau^{-1}(\omega)$ and $m^*(\omega)$ are shown in Fig. 14 for four metallic compositions. Except for $x=0.34$, singular, therefore physically insignificant ω dependences have to be assumed. These analyses suggest that the electronic state of the heavily doped CuO_2 plane might acquire the nature of a Fermi liquid.

The above conclusion is reinforced by the results of other experiments. We observe a very small or even negative-sign Hall coefficient for heavily doped samples, contrary to large and positive coefficients for lightly doped ones.[3,15] The negative sign is what one expects from the band calculation, and the small magnitude is an indication of a large Fermi surface and thus implies a breakdown of the hole picture doped into a CT insulator. In contrast to T-linear resistivity in the high-T_c regime, a quadratic temperature dependence shows up in the resistivity of heavily doped samples.[15] In nuclear quadrupole relaxation (NQR) measurements, a Korringa-type temperature dependence was found to dominate in the relaxation rate of Cu nuclear spins.[29] Furthermore, in Raman-scattering spectra, the anomalous electronic Raman continuum, as well as the contribution from spin fluctuation, is greatly suppressed.[20] All these properties are suggestive of the electronic structure with the character of a Fermi liquid. It should be noted that the change to these properties from those in the high-T_c regime occurs almost discontinuously at $x \sim 0.25$. As typically envisaged in the x dependence of N^*_{eff}, there seems to exist a discontinuity between the electronic structure of the high-T_c CuO_2 plane and that of the heavily doped CuO_2

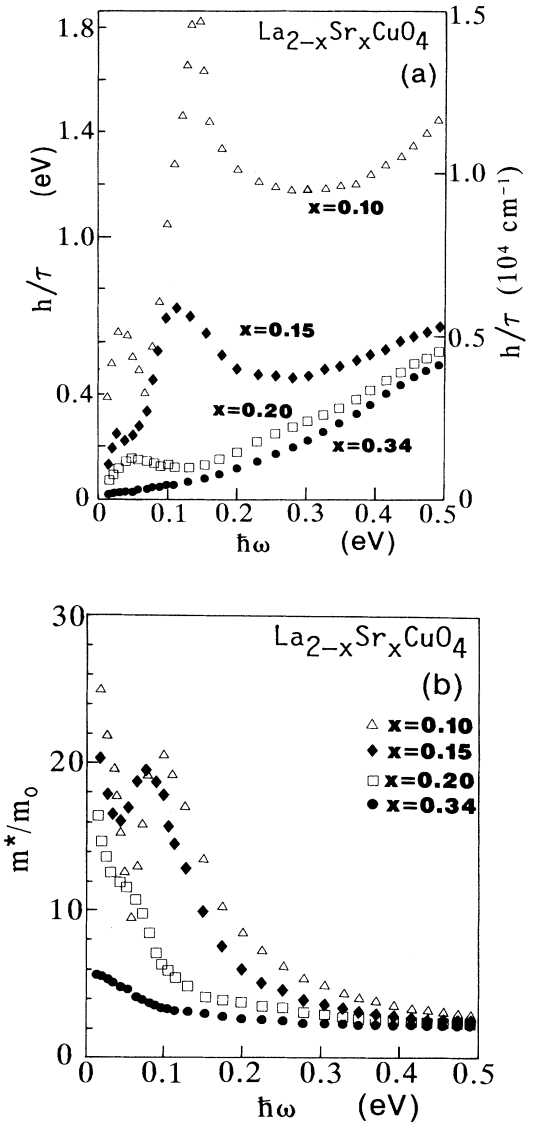

FIG. 14. (a) Energy-dependent scattering rate h/τ in eV (left) and in cm^{-1} (right), and (b) effective mass m^*/m derived from the complex conductivity $\hat{\sigma}(\omega)$ using an expression $\hat{\sigma}(\omega)=(ne^2/m)/[\tau^{-1}(\omega)-i\omega m^*(\omega)/m]$. $\hat{\sigma}(\omega)$ is obtained from the Kramers-Kronig transformation of the reflectivity data, and the value of n/m is set to be equal to N^*_{eff} (1.5 eV) for each x.

plane. Thus speculation might be made that the electronic state realized in the CuO_2 plane in the high-T_c regime can never be reached by a continuous extrapolation from a Fermi-liquid state.

D. Origin of the mid-IR band

Concerning the origin of the broadband of $\sigma(\omega)$ in the mid-IR region, several speculations have been made which include an incoherent motion of doped carriers against the background of anitferromagnetic spin fluctuation (t-J model),[30-34] spin- and/or charge fluctuation with a gap (or pseudogap) spectrum,[8,35] an optical transition involving midgap (or impurity) states created within the CT gap,[36] etc. The present results do not give conclusive evidence for either of these models but give constraints to them.

Midgap states are supposed to be formed just above the top of the occupied O $2p$ band like an acceptor impurity band in a semiconductor. Then two optical transition processes would give evidence for such states: One is the transition from the midgap states to the empty Cu $3d$ upper Hubbard band and the other from the O $2p$ to the midgap states. The former has been assigned to the 1.5-eV absorption reported by Suzuki on $La_{2-x}Sr_xCuO_4$ thin films,[19] and consequently the mid-IR absorption band has been identified as the latter process. The present work, however, does not favor this interpretation. The 1.5-eV absorption is a minor effect as compared with the mid-IR one, possibly extrinsic in origin, and is found to be quite specific to the $La_{2-x}Sr_xCuO_4$ system. Moreover, in this model it appears difficult to explain the observed rapid collapse of the CT excitation associated with rapid growth of the mid-IR absorption band.

A viewpoint of the gap excitation associated with spin(charge) fluctuation is related to the observation of a spin-excitation gap in the inelastic-neutron scattering experiment[24] as well as to the spin-excitation continuum observed up to ~ 1 eV in the Raman-scattering spectrum. Practically, this appears to be not the case. The present result emphasizes that the spectral weight of the mid-IR band is transferred from the CT excitation and eventually forms a single intraband excitation band together with the lowest-energy Drude-type absorption.

In this connection we should remark on a phenomenological argument, marginal Fermi liquid, made by Varma *et al.*[37] They identified the mid-IR absorption as the same origin as the electronic Raman continuum,[20] since they considered that both were derived from the common response function, the electrical polarizability $P(0,\omega)$. For high energies the Raman intensity is $I(\omega)\sim -\mathrm{Im}[1/\epsilon(\omega)]\sim -\mathrm{Im}P(0,\omega)$ and the optical conductivity was assumed to be given by $\sigma(\omega)=\omega\,\mathrm{Im}\epsilon(\omega)\sim -\omega\,\mathrm{Im}P(0,\omega)$. The IR spectra presented here together with the Raman spectra measured by Sugai *et al.*[20] on the same set of crystals provide a check at least to the above argument, although we do not doubt that the mid-IR band and the electronic Raman continuum have common origin in the unusual electronic structure of the CuO_2 plane. For small x we have seen that the loss function obtained from the KK analysis is featureless, but substantially large in the mid-IR region, coincident with a large and featureless Raman background in the same energy region. So it is possible that we are observing the same response from the electronic structure in the IR and Raman spectrum. On the other hand, for large x, including the high-T_c regime $\mathrm{Im}[-1/\epsilon(\omega)]$ exhibits a pronounced peak at $\omega\sim\omega_p$, while it is suppressed in the lower-energy region, very different from the observed Raman spectrum, which still shows a featureless continuum, though appreciably reduced. Such a spectral feature of $\mathrm{Im}(-1/\epsilon)$ arises from the strong ω dependence of the real part of $\epsilon(\omega)$. $\mathrm{Re}\epsilon(\omega)$ crosses zero near ω_p and has a large negative value at $\omega<\omega_p$ [$\mathrm{Im}(-1/\epsilon)=\epsilon_2/(\epsilon_1^2+\epsilon_2^2)$, ϵ_1 and ϵ_2 being the real and imaginary parts of ϵ, respectively]. This is much like the $\epsilon_1(\omega)$ of usual metal. Thus we are observing a different response in the $\sigma(\omega)$ spectrum from that in the Raman spectrum for the moderately or heavily doped CuO_2 plane. This is not surprising, considering that the electronic structure of the doped CuO_2 plane asymptotically approaches that of usual metal as x increases.

The optical conductivity has been calculated by several groups based on the t-J model by investigating carrier dynamics in a two-dimensional Mott-Hubbard insulator.[30-34] The energy of a doped hole is shown to be strongly renormalized because of the interactions with fluctuations of the surrounding spin system. A consequence of the interactions is a formation of coherent quasiparticle states with narrow width (an order of exchange energy J), which might correspond to the observed Drude-type absorption band. Above the coherent band there exists an incoherent band of states with strongly diffusive character due to scattering by spin fluctuations extending up to the energy of an order of the Cu-O transfer energy t. The mid-IR broadband absorption may be associated with this incoherent band. The calculated $\sigma(\omega)$ mimics the features of the observed spectrum of the doped CuO_2 plane as well as x dependence of the low-energy spectral weight to some extent. However, the relevance to the CT excitation which as observed here, transfers its spectral weight to the low-energy excitations with doping is far from clear. The doping-induced change of the electronic structure practically takes place over an energy range $\sim\Delta$; beyond that ($\sim J$) the t-J model can be dealt with.

We have supposed a situation as illustrated in Fig 13(e), which might be relevant to the mid-IR absorption, by considering the fact that both Cu $3d$ and O$2p$ states are involved in it and that it will eventually become intraband absorption in a Cu $3d$–O $2p$ hybridized band. This diagram is not real, representing one aspect of the actual electronic structure in that it ignores the excitations at lower energies, e.g., that responsible for the Drude-type absorption, but it becomes more substantial as the dopant concentration increases.

A similar picture has been drawn by the recent photoemission experiments of Namatame *et al.*[38] and by Allen *et al.*[39] on both $La_{2-x}Sr_xCuO_4$ and $Nd_{2-x}Ce_xCuO_4$. They found that the Fermi level is located at the same position in the CT gap for both hole and electron doping

and were led to the same conclusion as the present work that the states near the Fermi level are generated with doping by a transfer from both conduction- and valence-band states of the parent CT insulator. Allen *et al.* further argue that the entire gap of the undoped compound is filled with states on hole-electron doping and the gap-filling states might obey a Luttinger-type theorem at the Fermi energy. The present result does not fully agree with this argument in that the observed reflectivity edge near 0.8 eV may be regarded as a plasma edge resulting from intraband excitation across a Fermi surface of such a band of gap-filling states [as depicted in Fig. 13(e)], but the number of states enclosed within this Fermi surface would be appreciably smaller than that expected from the Luttinger sum rule, as deduced from the result of $N^*_{\rm eff}(\omega)$, which indicates remnant spectral weight in the CT excitation region.

V. SUMMARY

An almost complete set of the optical spectra of $La_{2-x}Sr_xCuO_4$ single crystals is presented in this paper by studying the x dependence over a wide compositional range $0 \le x \le 0.34$ and over a side energy range 0.004 eV $\le E \le 35$ eV. The spectra are also shown for light polarization perpendicular to CuO_2 planes ($E \| c$) for a few representative compositions. Such a systematic study is so far possible only for $La_{2-x}Sr_xCuO_4$ because x or a dopant concentration can be varied so as to cover all three fundamental phases, AF insulator, high-T_c superconductor, and normal metal, which are believed to appear in all layered copper oxides. Moreover, La_2CuO_4 has the simplest crystal structure with a single CuO_2 plane in a structural unit, and the optical response from the CuO_2 plane is observed below 3 eV, separated from the high-energy response from the LaO double layers. Thus it is possible to obtain unambiguous spectra of optical excitations associated with the CuO_2 plane and hence to characterize optically the electronic structures of the undoped and hole-doped CuO_2 plane where the high-T_c superconductivity is realized in all the known cuprates. The spectral features and thus characterized electronic structure of the CuO_2 plane are summarized for respective compositional region as follows.

A. Undoped CuO_2 plane ($x = 0$)

The spectrum is characterized by an excitonic absorption peak at 2 eV, which is assigned to O $2p \rightarrow$ Cu $3d$ charge-transfer excitation. The undoped CuO_2 plane is thus CT insulating with an optical gap of ~ 2 eV.

B. Lightly doped CuO_2 plane ($0 < x < 0.10$)

On doping low-energy excitations extending over the mid-IR region are evoked and they evolve by rapid transfer of the spectral weight from the CT excitation region. This indicates a redistribution of the Cu $3d$ and O $2p$ states on a large energy scale. The low-energy excitations are clearly separated into a Drude-type peak at $\omega = 0$ and a broadband centered in the mid-IR region. The mid-IR band is not a softened CT excitation, but is associated with the states created in the gap or incoherent motion of carriers with respect to the background spin system. The mid-IR band occupies most of the transferred spectral weight, hence giving rise to a quite unusual optical spectrum.

The Drude-type narrow band represents the (coherent) motion of doped *hole* carriers, as the spectral weight seems to increase proportionally with the dopant concentration x. This component is thus directly related to the dc transport properties. In fact, the Hall coefficient shows a decrease proportional to $1/x$ in the small x range. Thomas *et al.*[8] demonstrated, for $YBa_2Cu_3O_{6+x}$, that the width of the Drude-type peak is proportional to the thermal energy k_BT in coincidence with the T-linear resistity in the normal state.

C. Moderately doped CuO_2 plane ($0.10 \le x < 0.25$)

High-temperature superconductivity is observed in this range of dopant concentration. The transfer of the spectral weight becomes stationary against further increase of x, and the separation of the low-energy excitations into the two components in the $\sigma(\omega)$ spectrum is ambiguous as the Drude-type band rapidly grows and the mid-IR band shifts its center to lower energies. The low-energy excitations, as a whole, form a spectrum indicative of an electronic state of much enhanced itinerant character with spectral intensity biased more on the lower-energy region. This is also inferred from the real part of the dielectric function as well as the loss function $\mathrm{Im}[-1/\epsilon(\omega)]$. The former crosses zero at ω_p (~ 0.8 eV, corresponding to the reflectivity edge), and the latter shows a pronounced, though too broad, peak at $\sim\omega_p$, similar to the behavior that usual metals show at the plasma edge. From this, together with much increased spectral weight, one may conclude that not only O $2p$ states but also part of localized Cu $3d$ states contribute to the itinerant motion of carriers; that is, more degrees of of freedom than x holes take part in the dynamical charge motion in the high-T_c regime. The very small Hall coefficient, much smaller than V/xe, gives support to this conclusion.

Although the transfer of the spectral weight is saturated, a finite but appreciable weight remains in the CT energy region, so that the states near the Fermi energy do not achieve full itinerancy, some states being still localized. This fact appears to be connected with the short-range dynamical spin correlation observed in the NQR (Ref. 29) and inelastic-neutron scattering experiments.[24,25] It is noteworthy that the $E \| c$ ($\perp$ CuO_2 plane) spectrum is typical of insulators or semiconductors, almost unchanged from that for an undoped compound. Such a peculiar situation, metallic in one direction and insulating in the other, is evidence that the low-energy excitations are confined to the CuO_2 plane.

D. Heavily doped CuO_2 plane ($0.25 < x$)

The spectral weight of the CT excitation spreads over a wide energy range, no longer confined below 1.5 eV. The

low-energy excitations form a single band, which can be described by a generalized Drude formula with ω-dependent scattering time and effective mass as in the case of heavy-fermion superconductors. The spectrum suggests that the electronic state of the heavily doped CuO_2 plane acquire the nature of Fermi liquid. Very small, even negative-sign Hall coefficients[3,15] as well as a Korringa-type relaxation of the Cu nuclear spins,[29] support this conclusion. The notable fact is that the change from the high-T_c regime to this Fermi-liquid region takes place almost discontinuously at $x \sim 0.25$. This seems to indicate that the electronic structure in the high-T_c regime is not continuously connected to the Fermi-liquid state with an increase of dopant concentration.

The present results are universal for any hole-doped cuprate superconductor, and even in the electron-doped material very similar spectral change has been observed. They have consistency with the dc transport properties, in particular the Hall coefficient, as well as with high-energy spectroscopic results such as photoemission, x-ray absorption,[40] and electron-energy-loss spectra.[41] They also sort out features relevant to the Raman, neutron, and MQR experiments, and so the present optical study contributes to drawing a unified picture of the electronic structure of the normal-state high-T_c cuprates and to give constraints to the theoretical models.

ACKNOWLEDGMENTS

The authors gratefully acknowledge enlightening conversations with A. Fujimori, M. Imada, H. Katayama-Yoshida, Y. Kitaoka, Y. Kuramoto, K. Miyake, T. Takahashi, and K. Ueda. This work was supported by a Grant-in-Aid for Scientifi Research from the Ministry of Education, Science, and Culture of Japan.

[1]A. Fujimori, E. Takayama-Muromachi, Y. Uchida, and B. Okai, Phys. Rev. B **35**, 8814 (1987).
[2]Y. Tokura, S. Koshihara, T. Arima, H. Takagi, S. Ishibashi, and S. Uchida, Phys. Rev. B **41**, 11 657 (1990).
[3]S. Uchida, H. Takagi, Y. Tokura, S. Koshihara, and T. Arima, in *Strong Correlation and Superconductivity,* edited by H. Fukuyama, S. Maekawa, and A. P. Malozemoff (Springer, Tokyo, 1989), pp. 194–203.
[4]T. Takahshi, in Ref. 3, pp. 311–320.
[5]C. G. Olson *et al.*, Science **245**, 731 (1989).
[6]G. Mante *et al.*, Z. Phys. B **80**, 181 (1990).
[7]J. C. Campuzano *et al.*, Phys. Rev. Lett. **64**, 2308 (1990).
[8]G. A. Thomas *et al.*, Phys. Rev. Lett. **61**, 1313 (1988); J. Orenstein *et al.*, Phys. Rev. B **42**, 6342 (1990).
[9]R. T. Collins, Z. Schlesinger, F. Holtzberg, P. Chaudari, and C. Field, Phys. Rev. B **39**, 6571 (1989); Z. Schlesinger *et al.*, *ibid.* **41**, 11 237 (1990).
[10]B. Koch, H. P. Geserich, and T. H. Wolf, Solid State Commun. **71**, 495 (1989).
[11]M. P. Petrov *et al.*, Zh. Eksp. Teor. Fiz. **50**, 25 (1989) [JETP Lett. **50**, 29 (1989)].
[12]Y. Tokura, J. B. Torrance, T. C. Huang, and A. I. Nazzal, Phys. Rev. B **38**, 7156 (1988).
[13]S. Tajima *et al.*, J. Opt. Soc. Am. B **6**, 475 (1989).
[14]M. K. Kelly, P. Barboux, J.-M. Tarascon, and D. E. Aspnes, Phys. Rev. B **40**, 6797 (1989).
[15]H. Takagi *et al.*, Phys. Rev. B **40**, 2254 (1989).
[16]J. B. Torrance *et al.*, Phys. Rev. B **40**, 8872 (1989).
[17]I. I. Mazin *et al.*, Pis'ma Zh. Eksp. Teor. Fiz. **47**, 94 (1988) [JETP Lett. **47**, 113 (1988)].
[18]K. Kamaras, S. L. Herr, C. D. Porter, N. Tache, and D. B. Tanner, Phys. Rev. Lett. **64**, 84 (1990).
[19]M. Suzuki, Phys. Rev. B **39**, 2312 (1989).
[20]S. L. Cooper and M. V. Klein, Comments Condens. Matter Phys. **15**, 99 (1990); S. Sugai, T. Ido, H. Takagi, S. Uchida, and M. Sato, Solid State Commun. **76**, 365 (1990).
[21]T. Ito, T. Ido, H. Takagi, and S. Uchida (unpublished).
[22]W. E. Pickett, Rev. Mod. Phys. **61**, 433 (1989).
[23]B. C. Webb, A. J. Sievers, and T. Mihalisin, Phys. Rev. Lett. **57**, 1951 (1986).
[24]G. Shirane *et al.*, Phys. Rev. Lett. **63**, 330 (1989).
[25]J. Rossat-Mignod *et al.*, in Dynamics of Magnetic Fluctuations in High T_c Materials, edited by G. Reiter, P. Horsch, and G. Psaltakis (Plenum, New York, in press).
[26]P. W. Anderson, Int. J. Mod. Phys. B **4**, 181 (1990).
[27]J. Orenstein, G. A. Thomas, D. H. Rapkine, A. J. Millis, L. F. Schneemeyer, and J. V. Waszczak, Physica C **153-155**, 1740 (1988).
[28]I. Terasaki, T. Nakahashi, S. Takebayashi, A. Maeda, and K. Uchinokura, Physica C **165**, 152 (1990).
[29]Y. Kitaoka *et al.*, in Ref. 3, pp. 262–273; H. Yasuoka, T. Imai, and T. Shimizu, in *ibid.*, pp. 254–261.
[30]C. L. Kane, P. A. Lee, and N. Read, Phys. Rev. B **39**, 6880 (1989).
[31]T. M. Rice and F. C. Zhang, Phys. Rev. B **39**, 815 (1989).
[32]A. Moreo and E. Dagotto, Phys. Rev. B **42**, 4786 (1990).
[33]J. Inoue and S. Maekawa, J. Phys. Soc. Jpn. **59**, 2110 (1990).
[34]W. Stephan and P. Horsch, Phys. Rev. B **42**, 8736 (1990).
[35]C. M. Varma, S. Schmitt-Rink, and E. Abrahams, Solid State Commun. **62**, 681 (1987).
[36]M. Tachiki and S. Takahashi, Phys. Rev. B **38**, 218 (1988); T. Koyama and M. Tachiki, Physica C **162-164**, 1509 (1989).
[37]C. M. Varma, P. B. Littlewood, S. Schmitt-Rink, E. Abrahams, and A. E. Rukenstein, Phys. Rev. Lett. **63**, 1996 (1989).
[38]H. Namatame *et al.*, Phys. Rev. B **41**, 7205 (1990).
[39]J. W. Allen *et al.*, Phys. Rev. Lett. **64**, 595 (1990).
[40]N. Kosugi, H. Takagi, Y. Tokura, and S. Uchida (unpublished).
[41]H. Romberg, M. Alexander, N. Nucker, P. Adelmann, and J. Fink, Phys. Rev. B **42**, 8768 (1990).